THE JOURNAL OF PHYSICAL CHEMISTRY B

Article

pubs.acs.org/JPCB

Predictions of Phase Separation in Three-Component Lipid Membranes by the MARTINI Force Field

Ryan S. Davis[†]

Department of Physics, The University of Memphis, Memphis, Tennessee 38152, United States

P. B. Sunil Kumar

Department of Physics, Indian Institute of Technology Madras, Chennai- 600 036, India and MEMPHYS - Center for Biomembrane Physics, University of Southern Denmark, 5230 Odense, Denmark

Maria Maddalena Sperotto

CBS - Center for Biological Sequence Analysis, Department of Systems Biology, Technical University of Denmark, 2800 Kgs. Lyngby, Denmark

Mohamed Laradji*

Department of Physics, The University of Memphis, Memphis, Tennessee 38152, United States and MEMPHYS - Center for Biomembrane Physics, University of Southern Denmark, 5230 Odense, Denmark

ABSTRACT: The phase behavior of the coarse-grained MARTINI model for three-component lipid bilayers composed of dipalmytoyl-phosphatidylcholine (DPPC), cholesterol (Chol), and an unsaturated phosphatidylcholine (PC) was systematically investigated by molecular dynamics simulations. The aim of this study is to understand which types of unsaturated PC induce the formation of thermodynamically stable coexisting phases when added to mixtures of DPPC and Chol and to unravel the mechanisms that drive phase separation in such three-component mixtures. Our simulations indicate that the currently used MARTINI force field does not induce such phase separation in mixtures of DPPC, Chol, and unsaturated PCs with a low unsaturation level, such as palmitoyl-oleoyl-phosphatidylcholine (POPC) or dioleoyl-phosphatidylcholine (DOPC). Also, we found that phase separation does occur in mixtures of DPPC, Chol, and polyunsaturated PCs, such as dilinoleyl-phosphatidylcholine (DUPC) and diarachidonoyl-phosphatidylcholine (DAPC). Through systematic tweaking of the interactions between the hydrophobic groups of the PC molecules, we show that the appearance of phase separation in three-component lipid bilayers, as modeled through the MARTINI force field, is primarily due to the interactions between the coarse-grained molecules, i.e., the beads, rather than due to the differences between the conformations of saturated and unsaturated lipid acyl chains, namely entropy driven.

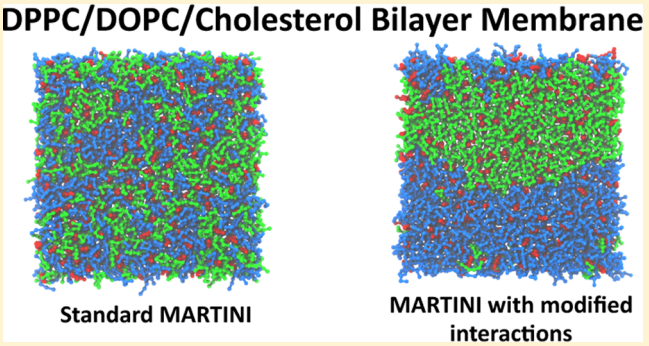

I. INTRODUCTION

It has been proposed that the plasma membrane of eukaryotic cells exhibits lateral heterogeneities, and it is suggested that among these are nanoscale cholesterol-enriched domains known as lipid rafts.[1] Lipid rafts are believed to be involved in many physiological processes including signaling,[2] trafficking,[3] caveolin-mediated endocytosis,[4] virus uptake,[5] and tension-regulation of the plasma membrane.[6,7] This view has challenged the fluid mosaic model of Singer and Nicolson[8] which proposes that the plasma membrane is a quasi-two-dimensional compositionally homogeneous fluid, which acts as a platform for membrane proteins. Understanding the nature of lipid rafts in plasma membranes is challenging and has been the subject of a large number of experimental and theoretical studies.[9−24]

Although recent *in vivo* studies using Förster's resonance energy transfer (FRET) reveal a nonrandom distribution of nanoscale clusters of GPI-anchored proteins, which further confirms the lipid raft hypothesis,[25,26] *in vivo* studies of the lateral organization of the plasma membrane are experimentally

Received: January 3, 2013
Revised: March 21, 2013
Published: March 27, 2013

dx.doi.org/10.1021/jp4000686 | *J. Phys. Chem. B* 2013, 117, 4072−4080

demanding. This is due to the fact that plasma membranes are very complex structures, made by a large number of lipid species and proteins. To overcome this difficulty, reconstituted model membranes are used to investigate, among others, the formation of lipid rafts. Examples of model membranes are giant unilamellar vesicles (GUVs) as well as planar bilayers composed of a saturated lipid, an unsaturated lipid, and Chol.[20] Experiments of reconstituted model membranes undergoing phase separation show that large segregated liquid-ordered (L_o) regions, rich in Chol and saturated lipids, coexist with large liquid-disordered (L_d) regions that are enriched in unsaturated lipids.[27−31] Since the length scale of these regions may extend up to the size of the reconstituted systems, one can view these segregated regions as phases separated in a thermodynamic sense. In the L_o phase, lipids exhibit high chain order but lack translational order, hence the term liquid-ordered is used to describe this phase, while lipids in the L_d phase lack both chain and translational order, hence the term liquid-disordered is used to describe this phase.

Binary mixtures of saturated and unsaturated lipids may exhibit thermodynamic coexistence between a L_d-phase, which is rich in the unsaturated lipid, and a solid (gel) ordered (S_o) phase, which is rich in the saturated lipid.[20,32] In contrast, liquid−liquid coexistence can appear in ternary lipid bilayers if the molecules of the third component, Chol, prefer to locate next to conformationally ordered lipid chains. This is due to the hydrophobically smooth and planar ring structure of Chol.[33] Therefore, Chol prefers locally lipid molecules with high chain order, readily provided by saturated lipids. Nevertheless, because of their shape and size, Chol molecules dissolve better in the laterally disordered L_d-phase. This unique nature of Chol[34] may explain why it induces the formation of what Ipsen et al.[35] defined as the liquid-ordered (L_o) phase.

Computational modeling and simulations have proven to be an indispensable tool in understanding both equilibrium and dynamic behavior of lipid membranes.[36,37] A number of coarse-grained computational models have been used to investigate the formation of lipid domains in multicomponent lipid membranes.[24] These include phase field models,[38,39] dynamic triangulation Monte Carlo models,[40] and particle-based coarse-grained models.[41−44] While these models may be a useful guideline for understanding the generic phase behavior of multicomponent lipid membranes, the understanding of system-specific properties necessitates detailed approaches such as atomistic molecular dynamics.

Few atomistic molecular dynamics (AMD) simulations of three-component lipid bilayers have thus far been performed.[45−48] A typical AMD simulation would involve a few thousand lipid molecules, corresponding to a linear system size which is smaller than a lipid raft. Furthermore, AMD simulations of lipid bilayers are only run over a few 100 ns. Thus, AMD can only probe short time-scale rearrangements of the lipid molecules.

Recently, Marrink et al. developed a system-specific coarse-grained force field,[49,50] known as the MARTINI force field, which is based on a four-to-one coarse-graining of heavy (carbon, oxygen, nitrogen, and phosphorus) atoms. According to this approach, a DPPC molecule, for example, is coarse-grained into 12 'beads'. The hydrophilic headgroup is composed of four hydrophilic beads and is connected to two semiflexible hydrocarbon chains, each composed of four hydrophobic beads. A trial-and-error procedure is used to optimize the parameters of the MARTINI force field in order to reproduce experimental densities of water and some alkanes at room temperatures. An extensive library for this force field has been developed and is being continuously upgraded for various types of lipids and amino acids.[50] The advantage of using the MARTINI model instead of AMD is that it both can be adopted for simulations of specific systems, and its time step can be 1 to 2 orders of magnitude larger than that in AMD, thus allowing for investigating larger systems and over longer time scales.

While phase separation has been experimentally observed in ternary mixtures of DPPC, dioleoyl-phosphatidylcholine (DOPC), and Chol,[30,51,52] so far only results for mixtures of DPPC/dilinoleyl-phosphatidylcholine (DUPC)/Chol and DPPC/diarachidonoyl-phosphatidylcholine (DAPC)/Chol have been reported using the MARTINI force field.[47,53] It is noted that DOPC has one unsaturated bond per chain. In contrast, both DUPC and DAPC are polyunsaturated, containing four and eight unsaturated carbon−carbon bonds, respectively. The following questions are therefore raised: Is it possible by the MARTINI approach to predict the occurrence of phase separation for the DPPC/DOPC/Chol? Also, what is the driving force of the phase separation in mixtures of DPPC, Chol, and polyunsaturated PCs? In order to answer these questions, we investigated systematically a number of three-component mixtures composed of DPPC, Chol, and unsaturated PC lipids with different levels of unsaturation. The simulations shown below refer to a temperature of 295 K. We found that with the current MARTINI parametrization, DPPC/palmitoyl-oleoyl-phosphatidylcholine (POPC)/Chol mixtures do not exhibit thermodynamically stable phase separation, in agreement with experiments.[27] However and in contrast to experimental results,[27,29,30,52] by using the MARTINI force field we cannot obtain phase separation in DPPC/DOPC/Chol mixtures. The absence of phase separation in the well-known raft mixture (DPPC/DOPC/Chol) within the MARTINI model may indicate that the phase separation in this model is not due to steric repulsion between unsaturated and saturated chains. We infer that phase separation in these ternary mixtures is mainly driven by interactions between the beads of the tail groups and is only very weakly dependent on differences between the conformational entropies of DPPC and the unsaturated PC lipids.

The remaining sections of this article are organized as follows. In section II, the MARTINI model is introduced, and the computational approach is presented. In section III, results are presented for the standard and modified MARTINI force field for DPPC/POPC/Chol, DPPC/DOPC/Chol, DPPC/DUPC/Chol, and DPPC/DUPC/Chol. A summary and concluding remarks are presented in section III.

II. MODEL AND COMPUTATIONAL METHOD

The MARTINI model is based on a four-to-one mapping of heavy atoms. Details of the model are presented in ref 50. Within this approach, the headgroup of a PC lipid molecule is composed of two types of coarse-grained beads corresponding to polar (Q) and nonpolar (N) beads. The tail group is composed of apolar (C) beads. MARTINI coarse-grained molecular structures of PC lipids used in the present study are shown in Figure 1. In DPPC, the all-saturated chains are composed of C1 beads. In either POPC or DOPC, beads containing unsaturated sites are represented by C3 beads. In either DUPC or DAPC, beads containing unsaturated sites are represented by C4 beads. Both C3 and C4 beads contain a

dx.doi.org/10.1021/jp4000686 | J. Phys. Chem. B 2013, 117, 4072−4080

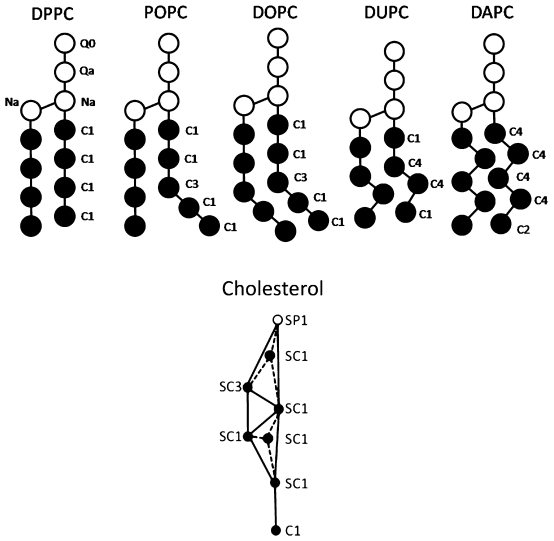

Figure 1. Top row: MARTINI's coarse-grained molecular structures of PC lipids used in the presented study shown with labeled particle types. The four types of lipid models share the same PC headgroup and have identical tails except for POPC. The bottom configuration is the MARTINI's coarse-grained molecular structure of cholesterol. Notice that C1, C2, C3, C4, SC1, and SC3 beads are hydrophobic. Interactions between these beads are shown in Tables 1 and 2.

single unsaturated bond and hence the same value of the bond angles at these sites. The remaining saturated sites in unsaturated PCs are either C1 or C2 beads, as depicted in Figure 1. Two-body interaction strengths between tail group beads are shown in Table 1. The present study is based on the MARTINI force field, version 2.1.

Table 1. Depth of the Lennard-Jones Potential Well, ε, between Different Types of Lipid Tail Beads Expressed in kJ/mol[a]

	C1	C2	C3	C4	C6
C1	ε = 3.5	3.5	3.5	3.1	3.5
C2	3.5	3.5	3.5	3.1	3.5
C3	3.5	3.5	3.5	3.5	3.1
C4	3.1	3.1	3.5	3.5	3.5
C6	3.5	3.5	3.1	3.5	3.5

[a]The length scale σ = 0.47 nm for all tail interactions. C1, C2, C3, and C4 are the coarse-grained beads as in the MARTINI model for the hydrocarbon chains. C6 beads are added as a replacement for the C1 beads which belong to DPPC. More details are presented in section II.B.

With regard to the modeling of water in the MARTINI force field, each coarse-grained water bead corresponds to four water molecules, but coarse-grained water beads are not polarizable. This is compensated for by implicit screening of the electrostatic interactions. While to neglect water polarization may be a reasonable approximation in the case of bulk water, this may not be so at the interface between water and the lipid bilayer head groups.[54] However, we do not expect the neglect of water polarization to directly influence lipid−lipid interactions.

The simulations were performed using the GROMACS software package,[55] version 4.0.7, and topology files provided in ref 56. The molecule types were separately coupled to a heat bath at 295 K and a pressure of 1 bar using the Berendsen thermostat and barostat with relaxation times of 1.0 and 2.0 ps, respectively. The barostats in the lateral and normal directions were decoupled with a compressibility equal to 3×10^{-4} bar^{-1} in both directions to simulate a tensionless bilayer. Simulations were run with a time step Δt = 0.02 ps over timelengths varying between 2 and 10 μs, depending on the time required to reach equilibrium as gauged by the total potential energy, bilayer area, and the net length of the interface between segregated domains.

Simulations are conducted on two bilayer sizes corresponding to 260 and 1040 molecules. These correspond respectively to linear dimensions approximately given by 8×8 nm^2 and 16×16 nm^2 and will be referred to herein as "small" and "large" systems, respectively. 2080 and 8320 solvent beads were used to hydrate the small and large systems, respectively. These correspond to eight coarse-grained solvent beads, or 32 water molecules, per lipid molecule. The bilayers were generated by initially distributing equal quantities of each lipid species randomly within each leaflet. The initial transbilayer lipid distribution is thus symmetric. Due to very rare lipid flip-flop events, this symmetric transbilayer lipid distribution is maintained throughout the simulation runs. Solvent beads were strictly placed in the spaces above and below the bilayer. After a short energy minimization, the simulations were begun with velocities randomly generated at 295 K, from a symmetric distribution of each component with zero mean. Where indicated, some systems were initiated with configurations taken from previously run simulations.

III. RESULTS

A. Domain Formation. Simulations were run for bilayers consisting of DPPC, unsaturated PC, and Chol with molar ratios of DPPC/unsaturated-PC/Chol corresponding to 35%/35%/30%. Four types of unsaturated lipids corresponding to POPC, DOPC, DUPC, and DAPC were used (cf. Figure 1).

Equilibrium snapshots (at 40 μs) of the four three-component bilayers are depicted in Figure 2. These snapshots

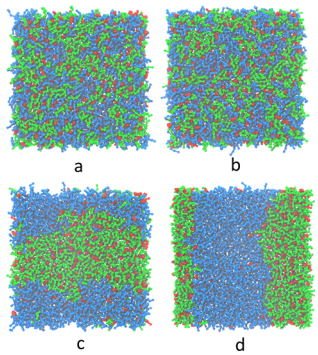

Figure 2. Equilibrium snapshots at 10 μs for ternary bilayers composed of DPPC, Chol and (a) POPC, (b) DOPC, (c) DUPC, and (d) DAPC at T = 295 K. Green particles belong to DPPC, blue particles belong to the unsaturated lipids, and red particles belong to Chol.

qualitatively demonstrate that ternary bilayers containing POPC or DOPC do not undergo phase separation. In sharp contrast to this, large domains form in the cases of DUPC and DAPC. Furthermore, Figure 2(c),(d) shows that the interfaces between segregated domains are rougher in the case of DUPC than in the case of DAPC. These qualitative results imply that, within the MARTINI approach, the degree of segregation

dx.doi.org/10.1021/jp4000686 | J. Phys. Chem. B 2013, 117, 4072−4080

between DPPC and the unsaturated PC increases with increasing the number of carbon−carbon double bonds in the unsaturated PC chains.

Figure 2(c),(d) also shows that Chol prefers to dissolve in the domains rich in DPPC and that Chol is more depleted from DAPC-rich regions than from DUPC-rich regions. The fraction of Chol molecules that have more DPPC neighbors than unsaturated PC neighbors, calculated using Voronoi diagrams, is shown in Figure 3 for the four studied mixtures. This figure

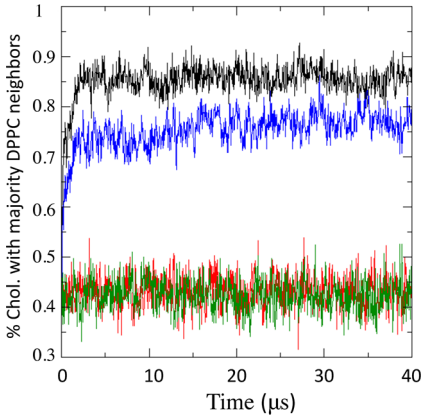

Figure 3. Fraction of Chol molecules that have more DPPC neighbors than saturated PC neighbors. The neighbors are determined using Voronoi diagrams. The Voronoi cells are calculated using the center of mass position of each molecule along the xy-plane. Curves from bottom to top correspond to the case where the unsaturated PC is POPC (black), DOPC (blue), DUPC (red), and DAPC (green), respectively. Note that the curves for POPC and DAPC are practically identical.

shows that the amount of Chol in DPPC-rich regions is highest in the case of DPPC/DAPC/Chol mixtures. Figure 3 also shows that in the cases of DPPC/POPC/Chol and DPPC/DOPC/Chol, the amount of Chol molecules that are mainly surrounded by DPPC molecules is low, essentially equal to the amount of Chol surrounded by either POPC or DOPC molecules.

Experimental evidence indicates that DPPC/POPC/Chol mixtures do not exhibit phase separation,[27] which is in agreement with the numerical predictions based on the MARTINI force field calculations. On the other hand, DPPC/DOPC/Chol mixtures have been shown experimentally to phase separate into large micrometer-scale domains,[27,30,51,52] which is in contrast with the results based on the MARTINI force field that we described above. We tested other DPPC/DOPC/Chol compositions of 40/40/20% and 30/30/40% and found similar results.

A finite size study is performed for all four mixtures over the small and large system sizes, in order to further characterize the nature of the phase separation in these systems. The finite size study will in particular allow to infer whether the large domains in DPPC/DUPC/Chol and DPPC/DAPC/Chol mixtures point to thermodynamic phase separation or are just thermal fluctuations. The amount of interface between two coexisting phases at equilibrium in a system of linear size L scales as $L^{\mathcal{D}-1}$, where $\mathcal{D}$ is the spatial dimension (in our case, $\mathcal{D} = 2$). Therefore, if a bilayer undergoes a thermodynamic phase separation, then the net interfacial length, $\mathcal{L}$, between the DPPC-rich and the unsaturated PC-rich domains should be proportional to the linear size, L, of the bilayer. In contrast, if the system remains mixed or exhibits some form of microphase separation, as it happens in the case of microemulsions, then the amount of interface between domains should be extensive, i.e. $\mathcal{L} \sim L^{\mathcal{D}}$.[57]

The interfacial length between DPPC-rich and unsaturated PC-rich domains was calculated using the edges of their Voronoi diagram with periodic boundary conditions. The lengths of edges that form the interface between unlike PC molecules are summed up in order to obtain $\mathcal{L}$. Chol is not accounted for in the determination of $\mathcal{L}$. Figure 4(a), where

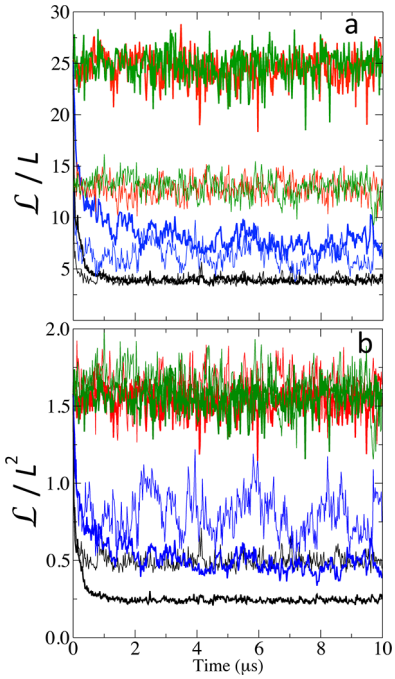

Figure 4. (a) Time dependence of the total interfacial length between DPPC rich and unsaturated PC-rich domains, normalized by the linear system size, $\mathcal{L}/L$, vs time. DPPC/DAPC/Chol is in black, DPPC/DUPC/Chol is in blue, DPPC/DOPC/Chol is in red, and DPPC/POPC/Chol is in green. Thin and thick curves correspond to the small and large systems, respectively. (b) Time dependence of the total interfacial length between DPPC rich and unsaturated PC-rich domains, normalized by the system's area, $\mathcal{L}/L^2$. Same colors and line thicknesses are used as in (a).

$\mathcal{L}/L$ is depicted for the four lipid mixtures, shows that $\mathcal{L}$ increases with increasing L for the cases of POPC and DOPC. Furthermore, Figure 4(b) shows that $\mathcal{L}/L^2 = 1.60$ and 1.62, in DPPC/POPC/Chol and DPPC/DOPC/Chol, respectively. This implies that within the MARTINI approach, both DPPC/POPC/Chol and DPPC/DOPC/Chol mixtures do not exhibit thermodynamic phase separation. This is consistent with the fact that the small domains in the snapshot of Figure 2(b) do not appear larger than those in Figure 2(a). Therefore, the difference between the structures of POPC's and DOPC's tail groups does not seem to affect the mixing/demixing behaviors of these mixtures.

In sharp contrast, Figure 4(a) demonstrates that $\mathcal{L}/L$ is independent of L for both DUPC and DAPC, implying that $\mathcal{L} \sim L$ in both these systems, and therefore both DPPC/DUPC/Chol and DPPC/DAPC/Chol mixtures exhibit thermodynamic phase separation. Furthermore, we note that $\mathcal{L}$ is

dx.doi.org/10.1021/jp4000686 | J. Phys. Chem. B 2013, 117, 4072−4080

higher for DUPC than DAPC, implying that the interfaces are rougher in the case of DUPC than in the case of DAPC. This is consistent with the shape of the interfaces in the snapshots of Figure 2(c),(d). This analysis implies that a relatively high level of unsaturation of PC lipids is required in the MARTINI model in order to produce thermodynamic phase separation.

B. Modified DPPC-DUPC and DPPC-DAPC Interactions. Having established in section III.A the miscibility of the DPPC/DOPC/Chol mixture with the current MARTINI parametrization, we now seek to answer why DPPC/DOPC/Chol fails to exhibit phase separation, in contrast to experimental evidence.[27,29,30,52] Figure 1 shows that in the MARTINI model, the beads containing double bonds in DUPC and DAPC, called C4, are different from the beads containing double bonds in POPC or DOPC, called C3. In particular, and as detailed in Table 1, the depth of the Lennard-Jones potential well of a C4−C1 pair, ε = 3.1 kJ/mol, is shallower than that of a C3−C1 pair, ε = 3.5 kJ/mol. Therefore DPPC-POPC or DPPC-DOPC interactions are less repulsive than DPPC-DUPC or DPPC-DAPC interactions. It is also important to note that within the MARTINI model, the depth of the well of a C1−C1 pair is equal to that of a C1−C3 pair. The following questions then arise: Are the phase separation in DPPC/DUPC/Chol or DPPC/DAPC/Chol and the lack of phase separation in DPPC/POPC/Chol or DPPC/DOPC/Chol the result of stronger structural differences between the MARTINI models for DPPC and DUPC or DAPC on one hand and POPC or DOPC on the other hand? Or are the occurrence or lack of phase separation rather due to the stronger repulsion between DPPC and DUPC or DAPC hydrocarbon beads when compared to that between DPPC and DOPC or POPC hydrocarbon beads?

It is noted that the strong similarity between the snapshots of DPPC/POPC/Chol and DPPC/DOPC/Chol, presented in Figure 2, and the corresponding normalized interfacial length, presented in Figure 4, imply that the difference in the saturation levels of POPC and DOPC, and corresponding difference in their molecular structures, do not lead to noticeable morphological differences between DPPC/POPC/Chol and DPPC/DOPC/Chol mixtures. It is also noted that as far as two-body interactions are concerned, all hydrophobic beads in POPC and DOPC are in fact identical to those in DPPC, namely they are C1 and C3 beads. Thus, within the MARTINI parametrization, the expected phase separation in DPPC/DOPC/Chol could only be conformationally driven. Therefore, would DPPC/DUPC/Chol and DPPC/DAPC/Chol still exhibit phase separation if the unsaturated beads in DUPC and DAPC are modified from C4 to C3 beads, similar to the unsaturated beads in POPC and DOPC?

In order to answer the question above, we modified DUPC and DAPC such that their unsaturated beads are similar to those in POPC and DOPC. This effectively means changing C4 beads into C3 beads but without affecting the interactions between DUPC molecules or between DAPC molecules (i.e., without compromising the properties of pure DUPC or DAPC). This is achieved by modifying C1 beads in DPPC to new beads, called C6, such that the C6−C4 interaction has the same strength as the C1−C3 interaction, as shown in Table 1. All other interaction parameters between C6 and other beads (including Chol beads) are the same as the interaction parameters between C1 and those other beads. It is noted that the length scale parameter, σ, in the Lennard-Jones potentials between hydrophobic beads is 0.47 nm regardless of the type of hydrophobic beads. Consequently, the σ-parameter is kept unmodified in this study. Furthermore, all parameters of the three-body interactions are also not modified in this study.

We performed simulations with the modified interaction parameters, where the initial conditions of the runs are equilibrium states, run with the conventional MARTINI parameters for 10 μs (see section III.A). The simulations with the new interaction parameters are run for another 5 μs.

The normalized interfacial length, $\mathcal{L}/L$, for both unmodified (0−10 μs) and modified (10−15 μs) DPPC/DUPC/Chol and DPPC/DAPC/Chol, are shown in Figure 5(c). The initial and final configurations for DPPC/DUPC/Chol after the modification of the interactions are shown in Figure 5(a),(b). Figure 5 shows that once the modification is made, the DPPC-rich and DUPC-rich or DAPC-rich domains become unstable leading to a breakdown in the relationship $\mathcal{L} \sim L$, implying a preference for mixing. Interestingly, the equilibrium domain structure of DPPC/DUPC/Chol, after modification of the interactions, becomes essentially identical to that of DPPC/DOPC/Chol. This is substantiated by the value of $\mathcal{L}/L \approx 25$ ($\mathcal{L}/L \approx 13$) in the large (small) system of the modified DPPC/DUPC/Chol mixture, which is equal to that of DPPC/DOPC/Chol, shown in Figure 4. Although the domains of DPPC/DAPC/Chol with modified interactions also break up, these domains are larger than those of DPPC/DUPC/Chol with modified interactions. This issue will be discussed later on.

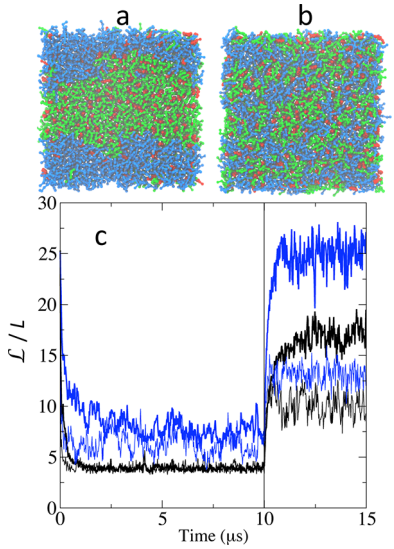

Figure 5. (a) Equilibrated snapshot at 10 μs of a DPPC/DUPC/Chol mixture without modified interactions. (b) Snapshot at 15 μs of the same mixture after modification of the C1−C4 interactions between DPPC and DUPC, at 10 μs, as explained in section III.B. (c) Amount of interfacial length between the unsaturated-rich and DPPC-rich domains, normalized by the linear size of the system, $\mathcal{L}/L$. Black and blue data correspond to DAPC and DUPC, respectively. Light (bottom) and bold (top) curves correspond to small and large systems, respectively.

The results above imply that the phase separation in DPPC/DUPC/Chol and DPPC/DAPC/Chol mixtures is the result of the C1−C4 interaction being more repulsive than the C1−C3 interaction, rather than the result of the structural differences between DPPC and DAPC or DUPC. We will see later that the larger domains in 'modified' DPPC/DAPC/Chol are the result

dx.doi.org/10.1021/jp4000686 | J. Phys. Chem. B 2013, 117, 4072−4080

of the more repulsive interaction between Chol and the C4 beads which has not been modified at this stage.

C. Modified DPPC-DOPC Interactions. In order to further infer the importance of the more repulsive C1−C4 interaction than the C1−C3 interaction, versus that of the differences between the conformations of DPPC and the unsaturated lipids, we effectively modified the C3 beads of DOPC into C4 beads, but in such a way that only interactions between the DPPC hydrocarbon beads and the DOPC hydrocarbon beads are affected, without compromising the properties of pure DOPC. As in the previous subsection, this is achieved by modifying the C1 beads in DPPC into C6 beads such that the depth of the C6−C3 interaction is equal to that of the C1−C4 interaction, as specified in Table 1.

Trajectories of $\mathcal{L}/L$ for DPPC/DOPC/Chol after modification for 5 μs and starting from an equilibrated configuration with conventional MARTINI's parameters is shown in Figure 6.

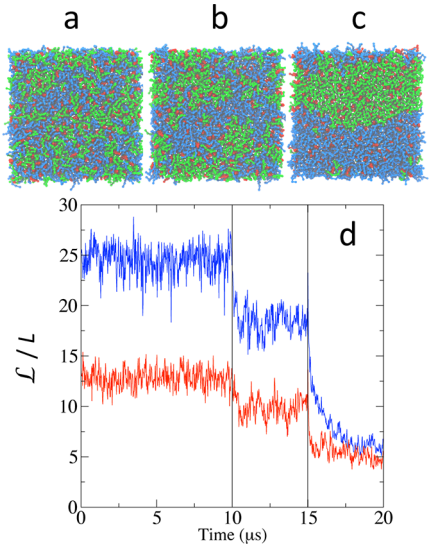

Figure 6. (a) Equilibrated snapshot at 10 μs of a DPPC/DOPC/Chol mixture without modified interactions. (b) Snapshot at 5 μs of the same mixture after modification of the unsaturated beads in DOPC into C1 beads, as explained in section III.C. (c) Snapshot after another 5 μs with modification of an additional C1 bead in DOPC into C4 beads. (d) Amount of interface between the unsaturated-rich and DPPC-rich domains, normalized by the linear size of the system, $\mathcal{L}/L$. Red and blue curves correspond to small and large systems, respectively.

In this figure, a set of snapshots after modification is also displayed. Figure 6(b) shows that making the DPPC-DOPC interaction more repulsive leads to larger domains. However, the ternary mixture fails from exhibiting a full phase separation, which implies that this change is not sufficient to induce phase separation. A lack of full phase separation is probably due to the fact that DOPC has now effectively only two C4 beads, while DUPC has four C4 beads and DAPC has eight C4 beads.

We therefore considered an additional, yet unrealistic, modification of DOPC tails by further modifying the second C1 beads in both DOPC's hydrocarbon tails from the end into C3 beads, while modifying all C1 beads of DPPC into C6 beads. This again ensures that the properties of pure DOPC are not affected by these modifications. The simulations were then run for another 5 μs (corresponding to the timespan 15−20 μs in Figure 6(d)). Interestingly, we found that, with this modification, the system undergoes a full phase separation, as shown by Figure 6(c), similar to that of DPPC/DUPC/Chol. These results therefore further solidify our conclusion that the phase separation in DPPC/saturated PC/Chol is the result of the more repulsive interaction between C1 and C4 beads when compared to that between C1 and C3 beads. In contrast, it seems that the difference in the conformations between DOPC and DUPC or DAPC does not seem to play a major role.

We note that here the interaction between Chol and DOPC has not been modified. This explains why the amount of Chol (red beads) in the DOPC-rich phase, as shown by Figure 6(c), is higher than that in the DUPC-rich or DAPC-rich phases with standard MARTINI parameters (cf. Figures 2(c) and 2(d)). It is anticipated that making the interaction between DOPC and Chol more repulsive might lead to full phase separation by simply modifying the two C3 beads into C4 beads in DOPC.

D. Modified Chol-DUPC and Chol-DAPC Interactions. Up to this point, we modified the interactions between the beads containing unsaturated bonds and the beads of DPPC, but we did not modify the interactions between Chol and the unsaturated beads of DUPC or DAPC. It is noted (see Table 2)

Table 2. Depth of the Lennard-Jones Potential, ϵ, between Different Types of Chol's Hydrophobic Beads and Lipid Hydrophobic Beads Expressed in kJ/mol[a]

	C1	C2	C3	C4	C6
SC1	ϵ = 3.5	3.5	3.5	3.1	3.5
SC3	3.5	3.5	3.5	3.5	3.5
SC6	3.5	3.5	3.5	3.5	3.5

[a]The length scale σ = 0.47 nm for all tail interactions. SC1 and SC3 are Chol's hydrophobic beads as indicated in Figure 1.

that the depth of the well of the interaction potential between SC1 beads in Chol and C4 beads in DUPC or DAPC is equal to that of the C1−C4 interaction, ϵ = 3.1 KJ/mol, which is more repulsive than the SC1-C1 and SC1-C3 interactions, with ϵ = 3.5 kJ/mol. This may explain why Chol tends to be depleted from regions rich in DUPC or DAPC but not from regions rich in DOPC, as shown by Figures 3 and 6(c).

To infer the role of Chol on the phase separation of DPPC/DUPC/Chol and DPPC/DAPC/Chol with the MARTINI force field, SC1 beads in Chol as well as C1 beads in DPPC are modified into SC6 and C6 beads, respectively. The strength of the interactions of SC6 beads with other tail beads are shown in Table 2. Note that the SC6 interaction with the C4 beads in DUPC and DAPC is of the same strength as the interaction between SC1 and C1 or C3 beads. The runs were again started from equilibrated configurations of DPPC/DUPC/Chol and DPPC/DAPC/Chol with standard MARTINI parametrization and subsequently run for 5 μs with modified interactions as outlined above.

Figure 7 shows that the additional modification of Chol's interaction with DUPC or DAPC makes the initial phase-separated domain structure even more unstable than in the case where only interactions between DPPC and DUPC or DAPC are modified (cf. section III B and Figure 5). In the case of DPPC/DAPC/Chol, a comparison between $\mathcal{L}/L$ in Figure 7(c) and that in Figure 5(c), where only DPPC-DAPC interactions are modified, shows that the domains are even smaller with the additional modification of the Chol-DAPC interaction. Furthermore, Figure 7(c) shows that the net interfacial length is practically identical for both DPPC/

dx.doi.org/10.1021/jp4000686 | J. Phys. Chem. B 2013, 117, 4072−4080

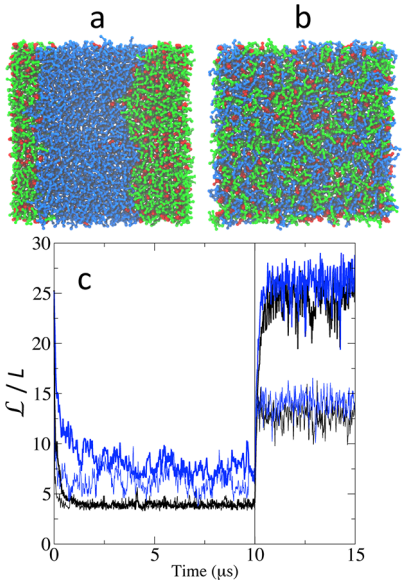

Figure 7. (a) Equilibrated snapshot at 10 μs of a DPPC/DAPC/Chol mixture without modified interactions. (b) Snapshot at 15 μs of the same mixture, i.e.,5 μs after modification of both DPPC saturated beads into C6 beads, and modification of SC1 beads in Chol into SC6 beads. With these modifications, the interaction C6−C4 is of the same strength as C1−C3, and the SC6-C4 is of the same strength as SC1-C3. (c) Net interfacial length between the unsaturated-rich and DPPC-rich domains, normalized by the linear size of the system, $\mathcal{L}/L$. Black and blue data correspond to DAPC and DUPC, respectively. Light (bottom) and bold (top) curves correspond to small and large systems, respectively.

DUPC/Chol and DPPC/DAPC/Chol, with the additional modification of Chol-DUPC or Chol-DAPC interactions, in contrast to the case where only DPPC-DUPC or DPPC-DAPC interactions are modified (cf. Figure 5(c)). Furthermore, $\mathcal{L}/L \approx 25$ or 13 for the large system or small system, respectively, for both cases of DPPC/DUPC/Chol and DPPC/DAPC/Chol with modified interactions. These values are the same as in the case of DPPC/POPC/Chol and DPPC/DOPC/Chol with standard MARTINI's parametrization (cf. Figure 4). Therefore, within the MARTINI modeling, the conformational differences, alone, between coarse-grained POPC, DPPC, DUPC, and DAPC do not have any effect on the partitioning of Chol in the different lipids and do not affect the phase separation in DPPC/unsaturated-PC/Chol mixtures. This implies that the domain segregation in coarse-grained DPPC/unsaturated-PC/Chol, within the MARTINI force field, is primarily driven by interactions between hydrophobic tail beads, rather than structural differences between DPPC and unsaturated PC molecules.

IV. SUMMARY AND CONCLUDING REMARKS

In this article, we have presented the results from a computational study of the phase separation of three-component lipid bilayers composed of DPPC, an unsaturated PC, and Chol. For this, we have adopted a molecular dynamics simulation method that is based on the coarse-grained MARTINI force field. Our aim was to investigate the effect of the PC's level of unsaturation on the phase behavior of the three-component bilayer. The unsaturated PCs we considered correspond to POPC, DOPC, DUPC, and DAPC, with each possessing one, two, four, and eight unsaturated carbon−carbon bonds, respectively.

Our simulations are performed in conjunction with a finite size analysis of the net interfacial length between DPPC-rich and DPPC-poor domains. We found that, with the current parametrization of the MARTINI force field, both DPPC/POPC/Chol and DPPC/DOPC/Chol mixtures do not exhibit thermodynamic phase separation, while both DPPC/DUPC/Chol and DPPC/DAPC/Chol mixtures do exhibit thermodynamic phase separation. We note that experimentally, the three latter mixtures do exhibit phase separation, while DPPC/POPC/Chol does not exhibit phase separation. While it is true that coarse-graining tends to underestimate conformational entropy of the system, and some parts of the interaction are incorporated as enthalpic, the question addressed in the current study is whether conformations play any role at all in the phase separation of ternary bilayers as described by the MARTINI force field.

Within the MARTINI force field approach, the interaction strength between the unsaturated beads, C3, of the hydrocarbon tails in POPC or DOPC and the saturated beads, C1, in DPPC is of the same strength as that between C1 beads. In contrast, the interaction between the unsaturated beads, C4, in DUPC or DAPC, and the saturated beads, C1, in DPPC is more repulsive than the C1−C3 interaction. It therefore appears that the phase separation in DPPC/DUPC/Chol and DPPC/DAPC/Chol might be entirely enthalpically driven.

To test this, we have modified the interaction strength between C1 and C3 beads to make it as repulsive as the C1−C4 interaction. Because of this modification, we found larger domains in DPPC/DOPC/Chol mixtures with this modification than with the current MARTINI parametrization. In contrast, by making the strength of the C1−C4 interaction, between DPPC and DUPC or DAPC, equal to that of the C1−C3 interaction, we found that DPPC/DUPC/Chol and DPPC/DAPC/Chol become mixed. These results indicate that phase separation in DPPC/unsaturated-PC/Chol, as predicted by the MARTINI force field simulations, is driven by the strength of the interaction between unsaturated beads and saturated beads, rather that differences between the conformations of the tail groups of DPPC and the unsaturated PC.

It is therefore legitimate to ask the following questions: What is the role, in the MARTINI force field, that the conformational differences between DPPC and the unsaturated PCs play? Also, does the MARTINI force field need a recalibration of the C1−C3 interaction in order to capture phase separation in DPPC/DOPC/Chol mixtures? It is understood that changing the C1−C3 interaction strength by making it more repulsive than the C1−C1 interaction will lead to more repulsive interactions between POPC molecules or DOPC molecules, thus increasing the area per lipid of a pure POPC or DOPC. This, however, can be taken care of by a simultaneous modification (reduction) of the parameter σ in the MARTINI force field.

AUTHOR INFORMATION

Corresponding Author

*Phone: 901-678-1676. E-mail: mlaradji@memphis.edu.

Present Address

[†]Department of Mechanical and Aerospace Engineering, Princeton University, NJ 08544, USA.

Notes

The authors declare no competing financial interest.

■ ACKNOWLEDGMENTS

We acknowledge funding from the National Science Foundation (DMR 0812470 and EPS 1004083). The authors would like to thank Profs. Martin J. Zuckermann and Yongmei Wang for useful discussions.

■ REFERENCES

(1) Pike, L. J. Rafts Defined: A report on the Keystone Symposium on Lipid Rafts and Cell Function. *J. Lipid Res.* **2006**, *47*, 1597−1598.
(2) Simons, K.; Ikonen, E. Functional Rafts in Cell Membranes. *Nature* **1997**, *387*, 569−572.
(3) Helms, J. B.; Zurzolo, X. Lipids as Targeting Signals: Lipid Rafts and Intracellular Trafficking. *Traffic* **2004**, *5*, 247−254.
(4) Van Mer, G.; Sprong, H. Membrane Lipids and Vesicular Traffic. *Curr. Opin. Cell Biol.* **2004**, *16*, 373−378.
(5) Chazal, N.; Gerlier, D. Membrane Lipids and Vesicular Traffic. *Microbiol. Mol. Biol. Rev.* **2003**, *67*, 226−237.
(6) Raucher, D.; Sheetz, M. P. Characteristics of a Membrane Reservoir Buffering Membrane Tension. *Biophys. J.* **1999**, *77*, 1992−2002.
(7) Sens, P.; Turner, M. S. Budded Membrane Microdomains as Tension Regulators. *Phys. Rev. E* **2006**, *73*, 031918.
(8) Singer, S. J.; Nicolson, G. L. Fluid Mosaic Model of Structure of Cell-Membranes. *Science* **1972**, *175*, 720−731.
(9) Coskun, Ü.; Simons, K. Membrane Rafting: From Apical Sorting to Phase Segregation. *FEBS Lett.* **2010**, *584*, 1685−1693.
(10) Wassal, S. R.; Stillwell, W. Polyunsaturated Fatty Acid-Cholesterol Interactions: Domain Formation in Membranes. *Biochim. Biophys. Acta* **2009**, *1788*, 24−32.
(11) Pike, L. J. The Challenge of Lipid Rafts. *J. Lipid Res.* **2009**, *50*, S323−S328.
(12) Jacobson, K.; Mouritsen, O. G.; Anderson, R. J. W. Lipid Rafts: at a Crossroad between Cell Biology and Physics. *Nat. Cell Biol.* **2007**, *9*, 7−14.
(13) Silvius, J. R.; Nabi, I. R. Fluorescence-Quenching and Resonance Energy Transfer Studies of Lipid Microdomains in Model and Biological Membranes. *Mol. Membr. Biol.* **2006**, *23*, 5−16.
(14) Hancock, J. F. Lipid Rafts: Contentious only from Simplistic Standpoints. *Nat. Rev. Mol. Cell Biol.* **2006**, *7*, 456−462.
(15) Munro, S. Lipid Rafts. *Cell* **2003**, *115*, 377−388.
(16) McMullen, T. P. W.; Lewis, R. N. A. H.; McElhaney, R. N. Cholesterol-Phospholipid Interactions, the Liquid-Ordered Phase and Lipid Rafts in Model and Biological Membranes. *Curr. Opin. Colloid Interface Sci.* **2004**, *8*, 459−468.
(17) Mayor, S.; Rao, M. Rafts: Scale-Dependent, Active Lipid Organization at the Cell Surface. *Traffic* **2004**, *5*, 231−240.
(18) Veatch, S. L.; Soubias, O.; Keller, S. L.; Gawrisch, K. Critical Fluctuations in Domain Forming Lipid Mixtures. *Proc. Natl. Acad. Sci.* **2007**, *104*, 17650−17655.
(19) Kusumi, A.; Koyama-Honda, I.; Suzuki, K. Molecular Dynamics and Interaction for Creation of Stimulation-Induced Stabilized Rafts from Small Unstable Rafts. *Traffic* **2004**, *5*, 213−230.
(20) Bagatolli, L. A.; Sunil Kumar, P. B. Phase Behavior of Multicomponent Membranes: Experimental and Computational Techniques. *Soft Matter* **2009**, *5*, 3234−3248.
(21) Foret, L. A Simple Mechanism of Raft Formation in Two-Component Fluid Membranes. *Europhys. Lett.* **2005**, *71*, 508−514.
(22) Laradji, M.; Sunil Kumar, P. B. Anomalously Slow Domain Growth in Fluid Membranes with Asymmetric Transbilayer Lipid Distribution. *Phys. Rev. E* **2006**, *73*, 040901−1 - 040901−4.
(23) Fan, J.; Han, T.; Haataja, M. Hydrodynamic Effects on Spinodal Decomposition Kinetics in Planar Lipid Membranes. *J. Chem. Phys.* **2010**, *133*, 235101.
(24) Laradji, M.; Sunil Kumar, P. B. Coarse-Grained Computer Simulations of Multi-Component Lipid Membranes. *Adv. Planar Lipid Bilayers Liposomes* **2011**, *14*, 201−232.
(25) Rao, M.; Mayor, S. Use of Forster's Resonance Energy Transfer Microscopy To Study Lipid Rafts. *Biochim. Biophys. Acta* **2005**, *1746*, 221−233.
(26) Chichili, G.; Rodgers, W. Cytoskeleton-Membrane Interactions in Membrane Raft Structure. *Cell. Mol. Life Sci.* **2009**, *66*, 2319−2328.
(27) Veatch, S. L.; Keller, S. L. Separation of Liquid Phases in Giant Vesicles of Ternary Mixtures of Phospholipids and Cholesterol. *Biophys. J.* **2003**, *85*, 3074−3083.
(28) Baumgart, T.; Hess, S. T.; Webb, W. W. Imaging Coexisting Fluid Domains in Biomembrane Models Coupling Curvature and Line Tension. *Nature* **2003**, *425*, 821−824.
(29) Veatch, S. L.; Keller, S. L. Miscibility Phase Diagrams of Giant Vesicles Containing Sphingomyelin. *Phys. Rev. Lett.* **2005**, *94*, 148101−1−148101−2.
(30) Yanagisawa, M.; Imai, M.; Komura, S.; Ohta, T. Growth Dynamics of Domains in Ternary Fluid Vesicles. *Biophys. J.* **2007**, *92*, 115−125.
(31) The fact that L_o domains in GUVs are orders of magnitude larger than lipid rafts in plasma membranes is not well understood and could be the result of critical fluctuations, various active processes such as lipid recycling or trafficking, cytoskeleton-induced confinement, or actively maintained transbilayer asymmetry in the lipid distribution.
(32) Stillwell, W.; Jenski, L. J.; Zerouga, M.; Dumaual, A. F. Detection of Lipid Domains in Docasahexaenoic Acid-Rich Bilayers by Acyl Chain-Specific FRET Probes. *Chem. Phys. Lipids* **2000**, *104*, 113−132.
(33) Hofsäß, G.; Lindahl, E.; Edholm, O. Molecular Dynamics Simulations of Phospholipid Bilayers with Cholesterol. *Biophys. J.* **2003**, *84*, 2192−2206.
(34) Mouritsen, O. G.; Zuckermann, M. J. What's so Special about Cholesterol? *Lipids* **2004**, *39*, 1101−1114.
(35) Ipsen, J. H.; Kalström, G.; Mouritsen, O. G.; Wennerström, H.; Zuckermann, M. J. Phase Equilibria in the Phosphatidylcholine-Cholesterol System. *Biochim. Biophys. Acta* **1987**, *905*, 162−172.
(36) Venturoli, M.; Sperotto, M. M.; Kranenburg, M.; Smit, B. Mesoscopic Models of Biological Membranes. *Phys. Rep.* **2006**, *437*, 1−54.
(37) Almeida, P. F. F. Thermodynamics of Lipid Interactions in Complex Bilayers. *Biochim. Biophys. Acta* **2009**, *1788*, 72−85.
(38) Taniguchi, T. Shape Deformation and Phase Separation Dynamics of Two-Component Vesicles. *Phys. Rev. Lett.* **1996**, *76*, 4444−4447.
(39) Fan, J.; Sammakorpi, M.; Haataja, M. Lipid Microdomains: Structural Correlations, Fluctuations and Formation Mechanisms. *Phys. Rev. Lett.* **2010**, *104*, 118101−1−118101−4.
(40) Sunil Kumar, P. B.; Gompper, G.; Lipowsky, R. Budding Dynamics of Multicomponent Membranes. *Phys. Rev. Lett.* **2001**, *86*, 3911−3914.
(41) Laradji, M.; Sunil Kumar, P. B. Dynamics of Domain Growth in Self-Assembled Fluid Vesicles. *Phys. Rev. Lett.* **2004**, *93*, 198105−1 - 198105−4.
(42) Laradji, M.; Sunil Kumar, P. B. Domain Growth, Budding, and Fission in Phase-Separating Self-Assembled Fluid Bilayers. *J. Chem. Phys.* **2005**, *123*, 224902.
(43) Cooke, I. R.; Kremer, K.; Deserno, M. Tunable Generic Model for Fluid Bilayer Membranes. *Phys. Rev. E* **2005**, *72*, 011506.
(44) Zheng, C.; Liu, P.; Li, J.; Zhang, Y.-W. Phase Diagrams for Multi-Component Membrane Vesicles: A Coarse-Grained Modeling Study. *Langmuir* **2010**, *26*, 12659−12666.
(45) Niemela, P. S.; Ollila, S.; Hyvonen, M. T.; Karttunen, M.; Vattulainen, I. Assessing the Nature of Lipid Raft Membranes. *PLoS Comput. Biol.* **2007**, *3*, 304−312.
(46) Berkowitz, M. L. Detailed Molecular Dynamics Simulations of Model Biological Membranes Containing Cholesterol. *Biochim. Biophys. Acta* **2009**, *1788*, 86−96.
(47) Apajalahti, T.; Niemala, P.; Govindan, P. N.; Miettinen, M. S.; Salonen, E.; Marrink, S. J.; Vattulainen, I. Concerted Diffusion of Lipids in Raft-Like Membranes. *Faraday Discuss.* **2010**, *144*, 411−430.

(48) Hall, A.; Róg, T.; Karttunen, M.; Vattulainen, I. Role of Glycolipids in Lipid Rafts: A View through Atomistic Molecular Dynamics Simulations with Galactosylceramide. *J. Phys. Chem. B* **2010**, *114*, 7797−7807.
(49) Marrink, S.; de Vries, A.; Mark, A. Coarse Grained Model for Semi-Quantitative Lipid Simulations. *J. Phys. Chem. B* **2004**, *108*, 750−760.
(50) Marrink, S.; Risselada, J.; Yefimov, S.; Tieleman, P.; de Vries, A. The MARTINI Force Field: Coarse Grained Model for Biomolecular Simulations. *J. Phys. Chem. B* **2007**, *111*, 7812−7824.
(51) Veatch, S. L.; Keller, S. L. Organization in Lipid Membranes Containing Cholesterol. *Phys. Rev. Lett.* **2002**, *89*, 268101−1−268101−4.
(52) Li, L.; Liang, X.; Lin, M.; Qiu, F.; Yang, Y. Budding Dynamics of Multicomponent Tubular Vesicles. *J. Am. Chem. Soc.* **2005**, *127*, 17996−17997.
(53) Risselada, H. J.; Marrink, S. J. The Molecular Face of Lipid Rafts in Model Membranes. *Proc. Natl. Acad. Sci.* **2008**, *105*, 17367−17372.
(54) Yesylevskyy, S. O.; Schäfer, L. V.; Sengupta, D.; Marrink, S. J. Polarizable Water Model for the Coarse-Grained Martini Force Field. *PLoS Comput. Biol.* **2010**, *6*, e1000810.
(55) Van Der Spoel, D.; Lindahl, E.; Hess, B.; Gorenhol, G.; Mark, A. E.; Berendsen, H. J. C. GROMACS: Fast, Flexible, and Free. *Comput. Chem.* **2005**, *26*, 1701−1718.
(56) The parameters of the MARTINI model version 2.1 are found in http://md.chem.rug.nl/cgmartini/index.php/downloads/force-field-parameters.
(57) Gompper, G.; Schick, M. In *Self Assembling Amphiphilic Systems*; Academic: New York, 1994.